Poly arginine-graphene quantum dots as a biocompatible and non-toxic nanocomposite: Layer-by-Layer electrochemical preparation, characterization and malondialdehyde sensory application in exhaled breath condensate

Mohammad Hasanzadeh [a*], Fozieh Mokhtari [b,c], Nasrin Shadjou [d,e,] Aziz Eftekhari [f], Ahad Mokhtarzadeh [g,b], Vahid Jouyban-Gharamaleki [h], Soltanali Mahboob [b]

Abstract

This study reports on the electropolymerization of a low toxic and biocompatible polymer with entitle poly arginine-graphene quantum dots (PARG-GQDs) as a novel strategy for surface modification of glassy carbon (GC) surface and preparation a new interface for biomedical application. The fabrication of PARG-GQDs on GCE was performed using Layer-by-layer regime. Scanning electron microscopy (SEM) was confirmed dispersion of GQDs on the surface of PARG which lead to increase of surface coverage of PARG. The redox behavior of prepared sensor was then characterized by cyclic voltammetry (CV), differential pulse voltammetry (DPV) and chronoamperometry (CHA), square wave voltammetry (SWV), linear sweep voltammetry (LSV). The electroactivity of PARG-GQDs coating towards detection and determination of malondialdehyde (MDA) as one of the most common biomarkers of oxidative stress, was then studied. Then, application of prepared sensor for the detection of MDA in exhaled breath condensate (EBC) is described. Electrochemical based sensor shows the lower limit of quantification (LLOQ) were 0.329 nanomolar. This work is the first report on the integration of GQDs to poly amino acids. Further development can lead to monitoring of MDA or other exhaled breath biomarkers by GQDs functionalized poly amino acids in EBC using electrochemical methods.

Keywords: conductive nano-material, graphene quantum dots; poly amino acid, biomarker, malondialdehyde; electrochemical sensor

1. Introduction

In recent decades, polymer films modified electrodes have been attracting vast attentions due to their broad applications in the fields of electrochemical sensors. [1] Such polymer films can notably improve the electroactivity properties of analytes, increase the reaction rate and improve the stability of the electrode response [2-7]. Up to now, various methodologies have been used to prepare polymer films modified electrodes, including coating [8, 9], covalent bonding [10] and electro-polymerization [11]. Among the methodologies, the electro-polymerization of organic molecules and especially amino acids with favorable functional groups (-COOH, -NH_2, -OH, -SH *etc.*) has showed evidence of to be an incredibly convenient means for preparing functionalized and electroactive polymers at electrodes surface, because the method can be conveniently controlled by adjusting the electrochemical factors. Accordingly, the thickness and charge transport characteristics of the modified electrodes by polymers can be well defined, and the cost of sensors is also low due to the easy electro-polymerization procedures [12-17].

Polymerizations of amino acids have attracted significant attention in the field of electrochemical sensors. The poly amino acid-modified electrodes were extensively used for the determination of various biomolecules and biomarkers [18, 19]. Owing to their broad applications, poly amino acid-modified electrodes have been prepared by electrochemical methods for electrochemical sensor applications [20-23] due to their excellent electroactivity properties. In recent years, poly-l-arginine (PARG)-modified electrodes have been extensively used in the electrochemical field and only a few reports were available in the sensor field. The PARG contains a guanidyl group, has a unique feature and could form electrostatic interactions with negatively charged groups of GQDs.

PARG modified electrode has been widely used to determine small biomolecules [24-28] for it includes guanidyl group which is engaged in hydrogen bonds with unique feature. Its multi-dentate characteristics enable L-arginine (ARG) to form long-range hydrogen-bonding and electrostatic interactions with negatively charged groups. [29].

In addition, PARG provided some amino groups for covalent modification, especially trouble-free for reaction with epoxy groups and carboxyl groups. One of the best candidates for this purpose is graphene quantum dots (GQDs). In the recent years, GQDs has become a promising class of the nano-carbon family, based on low toxicity, easy preparation, high chemical stability, environmental friendliness, and ability to transfer photoinduced electron [30, 31]. It has shown great promise applications in the fields of electrochemistry [32, 33]. GQDs can be functionalized [34] especially with oxygen containing groups such as hydroxyl, carboxyl and epoxy groups which can greatly enhance their hydrophilia and biocompatibility. Therefore, GQDs have considerable potential for electrochemical sensor applications. Consequently, incorporation of GQDs to the structure of electroactive polymers such as PARG can be increasing their electrical conductivity. These superior performances encouraged us to explore the possible leading role played by the presence of PARG decorated by GQDs which could increase the surface area of PARG to interact with some electroactive analytes. Since the increase in geometric surface area is very important parameter in electrochemistry, therefore modification of PARG with GQDs can enlarge the rate of electrochemical reaction. Therefore, addition of GQDs into PARG structure can be providing an electrically conductive thin film towards amplifies Faradic currents.

Excellent properties of PARG (its good biocompatibility and flexible structure framework) and the advantages of GQDs (low toxicity) have received our attention for preparation of high performance

and biologically friendly electrode material. It was for these reasons that we decided to explore the possibility of using the PARG functionalized by GQDs (PARG-GQDs) as a biocompatible environment platform for the development of electrochemical sensors. Considering that the electrochemical method possesses unique advantages for precise control over the redox reactions, we therefore hypothesize that, layer by layer electrochemical preparation of PARG-GQDs may provide an alternative approach for tailoring the surface properties of thin films. In summary, we investigated the electropolymerization of a low toxic and biocompatible polymer (PARG-GQDs) as a novel strategy for surface modification of glassy carbon surface. The formation of PARG-GQDs was firstly monitored. The latent reactivity of PARG-GQDs coating towards detection and determination of malondialdehyde (MDA) was then studied. The redox behavior of prepared sensor was then characterized by cyclic voltammetry (CV), differential pulse voltammetry (DPV) and chronoamperometry (CHA), square wave voltammetry (SWV), linear sweep voltammetry (LSV). Then, in continuation of our recent study concerning the malondialdehyde analysis using electrochemical sensor [35] as well as other reports by our research group [36-40], we used PARG-GQDs as a new biopolymer film for electro-oxidation and determination of this important biomarker. To the best of our knowledge, this is the first report of the layer-by-layer electrochemical preparation of PARG-GQDs films. In addition, this work is the first declaration on determination of malondialdehyde by poly amino acids functionalized by low toxic nano-material (GQDs).

2. Experimental

2.1. Chemicals & solutions

All chemicals used in this work were of analytical reagent grade. L-ARG was obtained from Sigma-Aldrich St. Louis, MO, USA). Additional dilute solutions were prepared daily by accurate dilution

just before use. MDA (produced from in situ hydrolysis of H_2SO_4) solutions were stable, and their concentrations did not change with time. Di-potassium phosphate and mono-potassium phosphate were obtained from Scharlau. Deionized water was purchased from Ghazi Pharmaceutical Company (Tabriz, Iran).

2.2. Cell culture

The human HepG2 cell lines were provided by the Institute of Pasture (Tehran, Iran). The cells were cultured in RPMI containing 10% (v/v) fetal bovine serum (FBS), antibiotics (Sigma-Aldrich, 50 U/mL penicillin and 50µg/mL streptomycin) and 2mM glutamine (Sigma-Aldrich St. Louis, MO, USA) under standard cell culture conditions (5% CO_2, 95% humidity and 37°C).

2.3. Cell viability assay

The cell viability was evaluated by the 3-(4, 5-dimethylthiazol) - 2-diphenyltetrazolium bromide (MTT) assay [41]. NIH-3T3 (mouse embryonic fibroblast cell line) and HepG2 (human liver cancer cell line) Cells were plated in 96-well microplates at a density of 3×10^4 and 1.2×10^4 cells per well respectively with 200 µl of the RPMI growth medium. All cells were incubated with various concentrations of graphene quantum dots (0, 10, 20, 50, 100, 200 ppm) over different incubation periods (24, 48, and 72 hours). After removing the medium, 50 µL of MTT solution (2 mg MTT/1mL PBS) was added to each well and were incubated for 4 hours at 37°C. Next, 25 µl ml Sorenson's glycine buffer (0.1 M glycine, 0.1 M NaCl, pH 10.5) and 200 µl DMSO were added to each well and after 30 min cell viability was determined by absorption measurement at 570 nm using a microplate reader (Biotek, ELx800, USA)

2.4. Instrument

Electrochemical experiments were performed with a computer-controlled AUTOLAB system with PGSTAT302N (Eco Chemie, Utrecht, The Netherlands), driven with NOVA 1.7 software. A conventional three-electrode cell was used with an Ag/AgCl (Methrom, The Netherlands) as a reference electrode, and a Pt wire was used as a counter-electrode. The working electrode was GCE (d=2mm) (from Azar electrode Co., Iran). For DPV measurements, a pulse width of 25 mV, a pulse time of 50 ms, and a scan rate of 50 mVs^{-1} were employed. The surface morphology of the modified electrodes was evaluated with a MIRA3 FEG-SEM (SEM, Hitachi Ltd., Czech,).

2.5. Preparation of EBC samples

EBC samples were obtained from healthy volunteers using a lab-made setup based on a cooling trap system patented in the national patent office. The setup cools down the exhaled breath down to -25 ºC and condenses the EBC with acceptable efficiency. 2.0 mL EBC sample collected from a healthy volunteer was transferred to a 10.0 mL volumetric flask, a standard solution of desired concentration was added up to the mark line, and electrochemical analysis was performed.

3. Results and discussion

3.1. Electropolymerization of L-arginine (L-ARG) on the surface of GCE

Before to the electrode modification, the glassy carbon electrodes were polished with 0.3 and 0.05 µm alumina (Beuhler, USA) slurries, and then ultrasonically cleaned by water, ethanol, and water for 3 min, respectively. The electrode was allowed to dry in air. CV was used to form the preparation thin film of PARG on the surface of GCE. Fig. 1 shows the continuous cyclic voltammograms of electrochemical polymerization of L-ARG on the surface of GCE. PARG film-modified GCE (with 2 mm diameter) was fabricated by electrochemical polymerization of L-ARG at the GCE by cyclic voltammetric method in 0.1M phosphate buffer solution (PBS) containing 0.5 mM arginine at pH 7.4.

Electropolymerization was performed between the potential -1.5 to 2 V *vs.* Ag/AgCl at the scan rate of 100 mV/s in 10 cycles. During the polymerization process, indiscernible peaks started to appear after the 2nd cycle. An anodic peak at 1.41 V and a reduction peak at -0.48 V were observed due to the formation of PARG. The peak current increased with increase in the number of cyclic voltammetric scans indicating that an electro-conductive polymer film was formed on the electrode surface. Finally, the oxidation peak disappeared after complete formation of PARG film. It has been confirmed that monomer containing NH_2 can be electropolymerized at the surface of electrode to form a conducting film via covalent bond (C–N) between electrode and NH_2. L-ARG has two NH2 and two NH groups and that can easily be oxidized to produce $NH_2\cdot$ Covalent bond (C–N) is then formed by the free radical reaction of NH_2. with GCE surface with excellent stability. Therefore, the covalent bond (C–N) might be formed between carbon electrode and the α-amino group of arginine. In is important to point out that, during the high potential scan rate, the α-amino free radical will easily form and the polymerization of the poly amino acid film could be formed on the surface of GCE. The reaction mechanism may be described as scheme 1.

After 10 cycle of cyclic voltammetric sweeps, the electropolymerization procedure was finished and the polymer film electrode was washed with distilled water to remove the physically adsorbed material. Then the film electrode was transferred to an electrochemical cell and cyclic voltammetric sweeps were carried out to obtain electrochemical steady state. In order to confirm the formation of PARG on GCE, the cyclic voltammetric sweep was carried out in 0.1 M PBS (pH=7.4) in the range of -1 to +1 V at 100 mV/s. A broad cyclic voltammogram compared to blank was obtained which confirms the deposition of polymer film on the electrode surface.

3.2. Electrodeposition of GQDs on the surface of PARG modified GCE

At first, GQDs was synthesized and characterized according to our previous reports [42-46]. To determine the effects of GQDs-induced toxicity NIH-3T3 and *HepG2* cells were exposed to different concentrations of graphene quantum dot (0, 10, 20, 50,100 and 200 ppm) for 24, 48 and 72 hour. Figures 3 represent the impact of GQDs treatment on the viability of cancerous cell line (HepG2) (A) and non-tumorigenic cell line (NIH-3T3) (B). Assessment of cell viability by MTT reduction cell viability test revealed that the increasing doses of graphene quantum dot up to 200 ppm did not show any significant effects on cell death of both cell lines.

Cyclic voltammetry (CV) was carried out for the electrodeposition of GQDs on PARG modified GCE from GQDs aqueous solution (0.002 g/mL) in the potential range from 0 to 1.0 V at a scan rate of 100 mV/s. Finally, thin film of PARG-GQDs was obtained at the surface of GCE (See scheme 2).

3.3. Characterization of PARG-GQDs film coated on GCE

FEG-SEM images of PARG and PARG-GQDs modified GCE are shown in Fig. 5. PARG electropolymerized directly on GCE in the absence of GQDs as matrix displays a regular and patterned structure (Fig. 5A). If the GCE was coated with GQDs beforehand, a compact film of GQDs can be observed (Fig. 5B) which the following deposition of GQDs on the PARG modified GCE results in the formation of an interwoven net-like structure of PARG-GQDs with regularly morphology (Fig. 5C), providing an efficient interface for the following combination with MDA biomarker. Finally, these results confirmed that the GCE was coated by PARG-GQDs film, leading to the change in the surface activity of the electrode. Also, these results confirm that dispersion of GQDs on the surface of PARG was performed successfully. These observations suggest that the PARG film provides GQDs more uniform dispersion. Noticeably, GQDs play a key role in the formation of regular and high ordered PARG-GQDs composite film. On the one hand, amine-containing groups on

PARG can provide large amounts of active sites for GQDs deposition. Also, the electron withdrawing oxygen-containing groups on GQDs are also beneficial to the combination with PARG from the electrostatic point of view. Consequently, PARG form long-range hydrogen-bonding and electrostatic interactions with negatively charged groups of GQDs. On the other word, PARG supplies some amino groups for covalent modification, especially easy for reaction with hydroxyl and carboxyl groups of GQDs. Therefore, a biocompatible polymer (PARG-GQDs) can be fabricated on the surface of glassy carbon electrode.

In general, scheme 3 show the preparation steps of PARG-GQDs modified GC electrode.

3.4. Electrochemical behavior of the PARG and PARG-GQDs film

The electrochemical behavior of PARG and PARG-GQDs film coated on GCE was investigated in further detail. Electrochemical characterization of the prepared biosensor was investigated by DPV, SWV, LSV, as well as CV techniques. Fig. 6 compares the cyclic voltammetric response of the PARG-GQDs-GCE with PARG-GCE. The cyclic voltammograms of GCE, PARG-GCE and PARG-GQDs-GCE were recorded between -1.0 and 1.0 V using the scan rate of 100 mVs^{-1} in the 0.1 M PBS (pH=7.4) in the presence of MDA. As seen in Fig. 6, on the bare GCE electrode (curve a) no redox behavior was observed. On the other hand, as well as on the PARG-GCE and PARG-GQDs-GCE one pair redox peaks was appeared at about 0.97 V *vs.* Ag/AgCl. The comparison of recorded CVs using PARG-GCE and PARG-GQDs-GCE in the presence of MDA (Fig 6A) shows high oxidation peak current for PARG-GQDs-GCE than PARG-GCE which attribute to the anodic oxidation of MDA using PARG-GQDs-GCE. This observation is also attributed to the high conductivity and inherent ability of PARG. These results show the anodic peak current at the surface of PARG-GQDs-GCE is significantly enhanced while; the cathodic peak current was decreased considerably. Also, it's found

that, PARG-GQDs film could accelerate the rate of electron transfer of MDA and have good electroactivity for redox reaction of MDA than PARG-GCE. It is no doubt that GQDs play important role in the improvement of electrochemical activity of PARG towards electrooxidation of MDA. As a decisive electrical component in the biopolymer film, GQDs provides an enhancement for sensitive detection of MDA, meanwhile, PARG can amplify the electrochemical signals produced during the electrochemical sensing process. In one word, the synergetic effect of PARG and GQDs leads to a successful

The pH dependence of E_{pa} can be expressed by the recording of CVs in different pH of MDA. Because the surface of electrode was coverage with amine groups, a pH of around 5 is optimal for imine formation. In addition, at higher pH there is insufficient acid present and at lower pH the amine will be protonated rendering it unable to do a nucleophilic attack at the carbonyl carbon. Therefore, we except in the pH about 5, a different oxidation potential be observed. Obtained results confirm this phenomenon Fig. 7. It is important to point out that, an aldehyde group could never be attacked directly by a protonated amine. Any such reaction would have to involve transfer of the proton from the amine to the MDA first in order to free up a lone pair on nitrogen, which might then attack the carbonyl carbon.

Scan rate has a significant role in the electrochemical behavior of analytes on the electrode surface. Fig. 8A presents typical CV of a PARG-*GQDs*-GCE in 0.1 M PBS at physiological pH (7.4) in different potential scan rates from 2-1000 mV s^{-1}. The peak's currents are relative to sweep rates in the range of 400-800 mV s^{-1}, as shown in Fig. 8B, pointing to the electrochemical activity of the surface redox couple. From the slope of this lines and using:

$$I_p = \left(\frac{n^2F^2}{4RT}\right)\nu A\Gamma^* \quad (1)$$

where Γ^* is the surface coverage of the redox species, ν being the potential sweep rate and A is the electrode surface area ($A=\pi r^2=0.125$ cm ^{2}) [47,48] and taking average of both cathodic and anodic results, Γ^* values of around 1.26×10^{-8} (mol cm^{-2} have been derived. In addition Γ^* values of PARG was 9.88×10^{-9} mol cm^{-2}. These results show that, prepared nanocomposite PARG-*GQDs* has higher surface coverage than bare PARG.

Fig. 8A-D illustrates cyclic voltammograms of MDA using the PARG-*GQDs*-GCE recorded at different potential sweep rates. Fig. 8B indicates anodic peak currents increased linearly with the square root of the potential sweep rate (400-800 mVs^{-1}), which indicates a mass transfer-controlling process of oxidation *via* diffusion. In addition the value of the electron-transfer coefficient for the reaction can be obtained from the following equation: [49, 50]

$$Ep = \left(\frac{RT}{2\alpha F}\right)\ln v + cons\tan t \quad (2)$$

This is valid for a totally irreversible diffusion-controlled process. Using the dependency of anodic peak potential on the Neperian logarithm of the potential sweep rate (Fig. 8C), the value of the electron-transfer coefficient was obtained as 0.432.

Chronoamperometry, as well as cyclic voltammetry has been employed for the investigation of the electrooxidation process of MDA at the surface of with PARG-*GQDs*-GCE. Chronoamperograms were recorded by setting the working electrode potentials to desired values and were used to measure the rate constant on the modified surface. Fig. 9 shows single steps chronoamperograms for the

modified electrode in presence of MDA over a concentration range of 0.001-0.2 M. The plot of net current versus $t^{-1/2}$ which has been obtained by removing the background current by the point-by-point sub-traction method gives a straight line. This indicates that the transient current must be controlled by a diffusion process. By using the slopes of these lines; we can obtain the diffusion coefficients of the MDA according to the Cottrell equation: [51]

$$I = nFAD^{1/2}C^{*}\pi^{-1/2}t^{-1/2} \quad (4)$$

where D is the diffusion coefficient, and C* is the bulk concentration. The mean value of the diffusion coefficients of MDA was found to be 1.01×10^{-5} cm^2 s^{-1}.

Electrode stability related to the number of cycles was also checked as Fig. 10. As shown, with increase of the number of cycles to 100, the peak currents decrease very smoothly with error of 3.3% where in higher cycles is decreased remarkably, for example, in 100 cycles error percent is 49%. Results approve that the electrode is stable at least 100 replicate analysis.

Another advantage of the proposed modified electrode was that the resulting modified electrode showed good long term stability. Stability of the proposed electrode was tested by measuring the decrease in voltammetric current during repetitive DPV measurements of MDA with PARG-*GQDs*-GCE stored in solution or air. For example, this electrode, within 24 h, is used for the determination of 0.1 mM MDA in buffer solutions. Obtained results show that this electrode has remarkable stability without significant change in the voltammetric currents. When the electrode was stored in the atmosphere, the current response remained almost unchanged for about 11 day. Relative standard deviation (RSD) of repeated peak currents was (6.0 %). The high stability of the PARG-*GQDs*-GCE could be related to the strong affinity of GQDs for PARG and the low solubility of the PARG-*GQDs*-GCE in water. To check the inter-electrode reproducibility of the modified electrode, three modified

electrodes were tested simultaneously by recording DPVs in buffer solution, containing 0.1 mM of MDA. The relative standard deviation was 6.16%. Therefore, 0.1 mM imparts a suitable stability onto DPVs measurements of biomarker.

3.5. Analytical application

The calibration curve for MDA in PBS was obtained by differential pulse voltammetry (DPV). Fig. 11A shows typical DPV curves for different concentrations of MDA in PBS using PARG-GQDs -GCE. The dependency between peak current and low concentration of MDA was rectilinear for lower MDA within the range of 0.06-0.2 μM (with a regression equation of I (μA)=0.736C (μM)-1.195, R^2=0.9831, n=5. The lower limits of quantitation (LLOQ) were found to be 0.329 nM for peak MDA. Also, in high concentrations of MDA regression equation of I (μA) =0.0297 C(μM)-16.528, R^2=0.9938, n=5.

Monitoring of EBC can be applied to rapid, non-invasive analyses of MDA with the aid of electrochemical methods. Therefore, PARG-*GQDs*-GCE was used as an efficient sensor for the detection of MDA in EBC using DPV. Since the EBC of healthy people is not free from MDA, in order to determine its MDA concentration, a standard addition method was used to obtain the concentration of MDA in the EBC of healthy people. For this purpose, in a healthy EBC sample, three concentrations of MDA were applied by the standard addition method and DPVs were recorded at pH 7.4. Obtained results are given in Table 1.

To test the accuracy of this electrochemical method, the results were compared with the standard method and summarized in Table 2. It was obvious that the MDA content detected by proposed method was lower than that detected by ultraviolet-visible spectrophotometry. It may be due to rather

poor sensitivity and selectivity of ultraviolet-visible detection for MDA. Therefore, this method could be further developed for the clinical assay of intracorporeal MDA content.

4. CONCLUSION

In summary, a novel electrochemical sensor was developed for detection and quantification of the MDA using PARG-*GQDs* modified GC electrode. The use of *GQDs* resulted in a remarkable increase in the surface area and the active sites of the PARG modified electrode. Meanwhile, using *GQDs* the electrochemical signal of PARG-GCE was markedly amplified. By using PARG-*GQDs*-GCE, the sensor displayed a good sensitivity toward MDA electrooxidation with LLOQ about 0.329 nM and relative standard deviation of 1.14%. The modified electrode shows excellent electroactivity for MDA oxidation and minimizes surface fouling effects of MDA and their oxidation products. More importantly, the proposed nano-sensor was used for determination of MDA at physiological pH, without the necessity for sample pretreatment or any time-consuming extraction or evaporation steps prior to the analysis, with satisfactory analytical results. In addition, the engineered sensor was successfully applied for the measurement of MDA EBC as a real sample. It is expected that this biocompatible nanocomposite based sensor will provide a fast, inexpensive, eco-friendly sensitive and reliable sensing method for applications in different areas of clinical medicine. Finally, the results indicates *GQDs* essential role in the signal amplification of PARG which is important in electroanalytical chemistry. Therefore, the attachment of GQDs to structure of PARG provides new opportunities within the personal healthcare, fitness, forensics, homeland security, and environmental monitoring domains. Application of other poly amino acids modified by GQDs for sensitive determination of MDA is under study and will be presented in detail in our future reports.

Acknowledgments

We gratefully acknowledge the partial financial support by the Ministry of Health and Medical Education of Iran, Drug Applied Research Center Research Center (DARC), Tabriz University of Medical Sciences, Higher Education Institute of Rab-Rashid, Nano Technology Research Center, and Faculty of Chemistry, Urmia University, Pharmaceutical Analysis Research Center (PARC) Tabriz University of Medical Sciences and also Iran National Science Foundation (INSF) for financial and instrumental supporting of this research.

5. References

[1] C. Tang, N. Chen, X. Hu. Conducting Polymer Nanocomposites: Recent Developments and Future Prospects, Conducting Polymer Hybrids, Springer International Publishing, 2016, pp 1-44

[2] H. Hosseini, M. Behbahani, M. Mahyari, H. Kazerooni, A. Bagheri, A. Shaabani, Ordered carbohydrate-derived porous carbons immobilized gold nanoparticles as a new electrode material for electrocatalytical oxidation and determination of nicotinamide adenine dinucleotide, Biosens. Bioelectron 59 (2014) 412-417.

[3] M. Kalate Bojdi, M. H. Mashhadizadeh, M. Behbahani, A.Farahani, S. S. Hosseini Davarani, A. Bagheri, Synthesis, characterization and application of novel lead imprinted polymer nanoparticles as a high selective electrochemical sensor for ultra-trace determination of lead ions in complex matrixes, Electrochim. Acta 136 (2014) 59-65.

[4] M. Kalate Bojdi, M. Behbahani, M.H. Mashhadizadeh, A. Bagheri, S. S. Hosseiny Davarani, A. Farahani, Mercapto-ordered carbohydrate-derived porous carbon electrode as a novel electrochemical sensor for simple and sensitive ultra-trace detection of omeprazole in biological samples, Materi.Sci. Engin. C 48 (2015) 213-219.

[5]M. Kalate Bojdi, M. Behbahani, A. Sahragard, B. Golrokh Amin, A. Fakhari, A. Bagheri, A palladium imprinted polymer for highly selective and sensitive electrochemical determination of ultra-trace of palladium ions, Electrochimi. Acta 149 (2014) 108-116

[6] M. Kalate Bojdi, M. Behbahani, M. Najafi, A. Bagheri, F. Omidi, S. Salimi, Selective and Sensitive Determination of Uranyl Ions in Complex Matrices by Ion Imprinted Polymers-Based Electrochemical Sensor, Electroanalysis 27 (2015) 2458-2467.

[7] M. Kalate Bojdi, M. Behbahani,G. Hesam, M. H. Mashhadizadeh, Application of magnetic lamotrigine-imprinted polymer nanoparticles as an electrochemical sensor for trace determination of lamotrigine in biological samples, RSC. Adv 6 (2016) 32374-32380.

[8] H. Tang, F. Yan, P. Lin, J. B. Xu, H. L. W. Chan, Highly Sensitive Glucose Biosensors Based on Organic Electrochemical Transistors Using Platinum Gate Electrodes Modified with Enzyme and Nanomaterials, Adv. Funct. Mater 21 (2011) 2264-2272.

[9] J. Soleymani, M. Hasanzadeh, N. Shadjou, M. Khoubnasab Jafari, J. Vaez Gharamaleki, M. Yadollahi, A. Jouyban, A new kinetic-mechanistic approach to elucidate electrooxidation of doxorubicin hydrochloride in unprocessed human fluids using magnetic graphene based nanocomposite modified glassy carbon electrode, Mater. Sci. Engin: C 61 (2016) 638-650

[9] X. Wang, G. Li, L. Liu, Y. Cheng, W. Zheng, S. Wu, F. Wu, W. Sun, Application of titanium dioxide nanowires and electroreduced graphene oxide modified electrodes for the electrochemical detection of specific tlh gene sequence from Vibrio parahaemolyticus, Anal. Method 7 (2015) 2623-2629.

[9] W. Sun, X. Qi, Y. Chen, S. Liu, H. Gao, Application of chitosan/Fe_3O_4 microsphere-graphene composite modified carbon ionic liquid electrode for the electrochemical detection of the PCR product of soybean Lectin gene sequence, Talanta 87 (2011) 106-112.

[10] M. Hasanzadeh, S. Sadeghi, L. Bageri, A. Mokhtarzadeh, A. karimzadeh, N. Shadjou, S. Mahboob. Poly-dopamine-beta-cyclodextrin: A novel nanobiopolymer towards sensing of some amino acids at physiological pH. Materials Science and Engineering: C 69 (2016) 343-357

[10] S. Shahrokhian, M. Karimi, H. Khajehsharifi, Carbon-paste electrode modified with cobalt-5-nitrolsalophen as a sensitive voltammetric sensor for detection of captopril, Sensor. Actuator. B 109 (2005) 278-284.

[10] S. Shahrokhian, E. Asadian, Simultaneous voltammetric determination of ascorbic acid, acetaminophen and isoniazid using thionine immobilized multi-walled carbon nanotube modified carbon paste electrode, Electrochim. Acta 55 (2010) 666-672.

[11] K. Wang, Z. Sun, M. Feng, A. Liu, S. Yang, Y. Chen, X. Lin, Design of a sandwich mode amperometric biosensor for detection of PMLRAR fusion gene using locked nucleic acids on gold electrode, Biosens. Bioelectron 26 (2011) 2870-2076.

[12] S. Lupu, F.J. del Campo, F. X. Muñoz, Development of microelectrode arrays modified with inorganic-organic composite materials for dopamine electroanalysis, J. Electroanal. Chem 639 (2010) 147-153.

[13] S. Cosnier, Biosensors based on immobilization of biomolecules by electrogenerated polymer films, Appl. Biochem. Biotechnol 89 (2000) 127-138.

[14] M. Hasanzadeh, M.H. Pournaghi-Azar, N. Shadjou, A. Jouyban. Electropolymerization of taurine on gold surface and its sensory application for determination of captopril in undiluted human serum, Mater. Sci. Engin. C 38 (2014) 197-205

[15] B. Massoumi, S. Fathalipour, A. Massoudi, M. Hassanzadeh, A.A. Entezami. Ag/Polyaniline Nanocomposites: Synthesize, Characterization, and Application to the Detection of Dopamine and Tyrosine, J. App. Polym. Sci. 130 (2013) 2780-2789

[16] M. Zamani-Kalajahi, M. Hasanzadeh, N. Shadjou, M. Khoubnasabjafari, K. Ansarin, V. Jouyban-Gharamaleki, A. Jouyban. Electrodeposition of taurine on gold surface and electro-oxidation of malondialdehyde. Surf. Engin. 31(2015) 194-201.

[17] M. Hasanzadeh, A. Bahrami, M. Alizadeh, N. Shadjou, Magnetic nanoparticles loaded on mobile crystalline material-41: preparation, characterization and application as a novel material for the construction of an electrochemical nanosensor, RSC Adv. 3 (2013) 24237-24246

[18] R. Thangamuthu, Y.C. Pan, S.M. Chen, Iodate Sensing Electrodes Based on Phosphotungstate−Doped−Glutaraldehyde−Cross−Linked Poly−L−lysine Coatings, Electroanalysis 22 (2010) 1812-1816.

[19] S. Cheemalapati, S. Palanisamy, S.M. Chen, A simple and sensitive electroanalytical determination of anxiolytic buspirone hydrochloride drug based on multiwalled carbon nanotubes modified electrode, J. Appl. Electrochem. 44 (2014) 317-323.

[20] D.P. Santos, M.F. Bergamini, A.G. Fogg, M.V.B. Zanoni, Application of a glassy carbon electrode modified with poly (glutamic acid) in caffeic acid determination, Microchim. Acta 151 (2005) 127-134.

[21] M. Wei, S. Deng-Ming, Simultaneous Determination of Epinephrine and Dopamineat with Poly (L-arginine) Modified Electrode, Chin. J. Anal. Chem 35 (2007) 66.

[22] K. Zhang, P. Luo, J. Wu, W. Wang, B. Ye, Highly sensitive determination of Sunset Yellow in drink using a poly (L-cysteine) modified glassy carbon electrode, Anal. Methods 19 (2013) 5044-5050.

[24] B.N. Chandrashekar, B.E. Kumara Swamy, M. Pandurangachar, T.V. Sathisha, B.S. Sherigara, Electropolymerisation of L-arginine at carbon paste electrode and its application to the detection of dopamine, ascorbic and uric acid, Colloid. Surface B. 88 (2011) 413-418.

[25] Z. Wu, H. Zhao, Y. Xue, X. Li, Y. He, Z. Yuan, Simultaneous Determination of 3, 4-Dihydroxyphenylacetic Acid, Uric Acid and Ascorbic Acid by Poly (L-Arginine)/Multi-Walled Carbon Nanotubes Composite Film, J. nanosci. Nanotechnol 11 (2011) 1013-1018.

[26] W. Ma, D.M. Sun, Simultaneous determination of epinephrine and dopamine with poly (l-arginine) modified electrode, Chin. J. Anal. Chem 35 (2007) 66-70.

[27] F. Zhang, Z. Wang, Y. Zhang, Z. Zheng, C. Wang, Y. Du, W. Ye, Simultaneous electrochemical determination of uric acid, xanthine and hypoxanthine based on poly (l-arginine)/graphene composite film modified electrode, Talanta 93 (2012) 320-325.

[28] Q. Cao, H. Zhao, Y. Yang, Y. He, N. Ding, J. Wang, Z. Wu, K. Xiang, G. Wang, Electrochemical immunosensor for casein based on gold nanoparticles and poly (l-Arginine)/multi-walled carbon nanotubes composite film functionalized interface, Biosens. Bioelectron 26 (2011) 3469-3474.

[29] Z.H. Sun, W.M. Sun, C.T. Chen, G.H. Zhang, X. Q. Wang, D. Xu, L-Arginine trifluoroacetate salt bridges in its solid state compound: The low-temperature three dimensional structural

determination of l-arginine bis (trifluoroacetate) crystal and its vibrational spectral analysis, Spectrochim. Acta. A 83 (2011) 39-45.

[30] O. Lv, Y. Tao, Y. Qin, C. Chen, Y. Pan, L. Deng, L. Liu, Y. Kong, Highly fluorescent and morphology-controllable graphene quantum dots-chitosan hybrid xerogels for in vivo imaging and pH-sensitive drug carrier. Mater. Sci. Engin. C, 67 (2016) 478-485.

[31] J.Ou, Y.Tao, J. Xue, Y. Kong, J. Dai, Linhong Deng, Electrochemical enantiorecognition of tryptophan enantiomers based on graphene quantum dots-chitosan composite film. Electrochem. Commun. 57 (2015) 5-9

[32] J. Ou, Y. Zhu, Y. Kong, J. Ma, Graphene quantum dots/β-cyclodextrin nanocomposites: A novel electrochemical chiral interface for tryptophan isomer recognition. Electrochem. Commun. 60 (2015) 60-63

[33] J. Ou, Y. Tao, J. Ma, Y. Kong, Well-Dispersed Chitosan-Graphene Quantum Dots Nanocomposites for Electrochemical Sensing Platform. J. Electrochem. Soc. 162 (2015) H884-H889.

[34] Y. Yu, W. Liu, J. Ma, Y. Tao, Y. Qin, Yong Kong. An efficient chiral sensing platform based on graphene quantum dot–tartaric acid hybrids. RSC Advances, 6 (2016) 84127-84132

[35] M. Zamani-Kalajahi, M. Hasanzadeh, N. Shadjou, M. Khoubnasabjafari, K. Ansarin, V. Jouyban-Gharamaleki, A. Jouyban, Electrodeposition of taurine on gold surface and electro-oxidation of malondialdehyde, Surface. Eng 31 (2015) 194-201.

[36] M, Khoubnasabjafari, K. Ansarin, A. Jouyban, Critical review of malondialdehyde analysis in biological samples, Curr. Pharm. Anal 12 (2016) 4-17.

[37] M. Khoubnasabjafari, K. Ansarin, A. Jouyban, Variations of malondialdehyde in pre-eclampsia, Hypertens. Pregnancy 35 (2016) 1-4.

[38] M. Khoubnasabjafari, K. Ansarin, A. Jouyban. Reliability of Malondialdehyde Measurements as a Marker of Oxidative Stress in Pediatrics, Pediatrics & Neonatology 57 (2016) 450.

[39] M. Khoubnasabjafari, K. Ansarin, A. Jouyban, Comments Concerning "Comparison of Airway and Systemic Malondialdehyde Levels for Assessment of Oxidative Stress in Cystic Fibrosis", Lung 193 (2015) 867-868

[40] M. Khoubnasabjafari, M. Khalil Ansarin, A. Jouyban. Salivary malondialdehyde as an oxidative stress biomarker in oral and systemic diseases, J. Dent. Res. Dent. Clin. Dent. Prospects 10 (2016) 71–74.

[41] J. G. Wu, Y. J. Kan, Y. B. Wu, J. Yi, T. Q. Chen, J. Z. Wu. Hepatoprotective effect of ganoderma triterpenoids against oxidative damage induced by tert-butyl hydroperoxide in human hepatic HepG2 cells, Pharm. biol 54 (2016) 919-929.

[42] M. Hasanzadeh, A. Karimzadeh, N. Shadjou, A. Mokhtarzadeh, L. Bageri, S. Sadeghi, S. Mahboob. Graphene quantum dots decorated with magnetic nanoparticles: Synthesis, electrodeposition, characterization and application as an electrochemical sensor towards determination of some amino acids at physiological pH, Mater. Sci. Eng C. 68 (2016) 814-830.

[43] N. Shadjou, M. Hasanzadeh, M. Marandi, A. Hasanzadeh. Graphene quantum dot functionalized by chitosan as an electrically conductive nano-material toward low potential detection: a new platform for interface science, J. Mater. Sci 27 (2016) 11834-11843.

[44] N. Shadjou, M. Hasanzadeh, F. Talebi, A. Poursattar Marjani. Integration of β-cyclodextrin into graphene quantum dot nano-structure and its application towards detection of Vitamin C at physiological pH: A new electrochemical approach, Mater. Sci. Eng. C 67 (2016) 666-674.

[45] M. Hasanzadeh, Mohammad, N. Hashemzadeh, N. Shadjou, J. Eivazi-Ziaei, M. Khoubnasabjafari, A. Jouyban. Sensing of doxorubicin hydrochloride using graphene quantum dot modified glassy carbon electrode, J. Mol. Liq 221 (2016) 354-357.

[46] M. Hasanzadeh, N. Shadjou, M. Marandi. Graphene quantum dot functionalized by chitosan and beta-cyclodextrin as a new support nanocomposite material for efficient methanol electrooxidation, J. Alloy. Compd 688 (2016) 171-186.

[47] A.L. Liu, S.B. Zhang, W. Chen, X.H. Lin, X.H. Xia, Poly(pyrocatechol-3,5-disodiumsulfonate)/ multi-walled carbon nanotubes composite for simultaneous determination of dopamine, ascorbic acid and uric acid, J. Nanosci. Nanotechnol. 13 (2013) 1563-1568.

[48] P. Gan, J. S. Foord, R. G. Compton, Surface Modification of Boron−Doped Diamond with Microcrystalline Copper Phthalocyanine: Oxygen Reduction Catalysis, Chem.Open (2015) 606-612.

[49] L. Zhou, J.D. Glennon, J.H. T. Luong, F.J. Reen, F. O'Gara, C. McSweeney, G.P. McGlacken, Detection of the pseudomonas quinolone signal (PQS) by cyclic voltammetry and amperometry using a boron doped diamond electrode, Chem.Commun 47 (2011) 10347-10349.

[50] R. S. Nicholson, I. Shain, Theory of stationary electrode polarography: single scan and cyclic methods applied to reversible, irreversible, and kinetic systems, Anal. Chem 36 (1965) 706-723.

[51] A.J. Bard, L.R. Faulkner, Electrochemical Methods: Fundamentals and Applications second ed., 236, John Wiley & Sons, New York, 2001, p. 503.

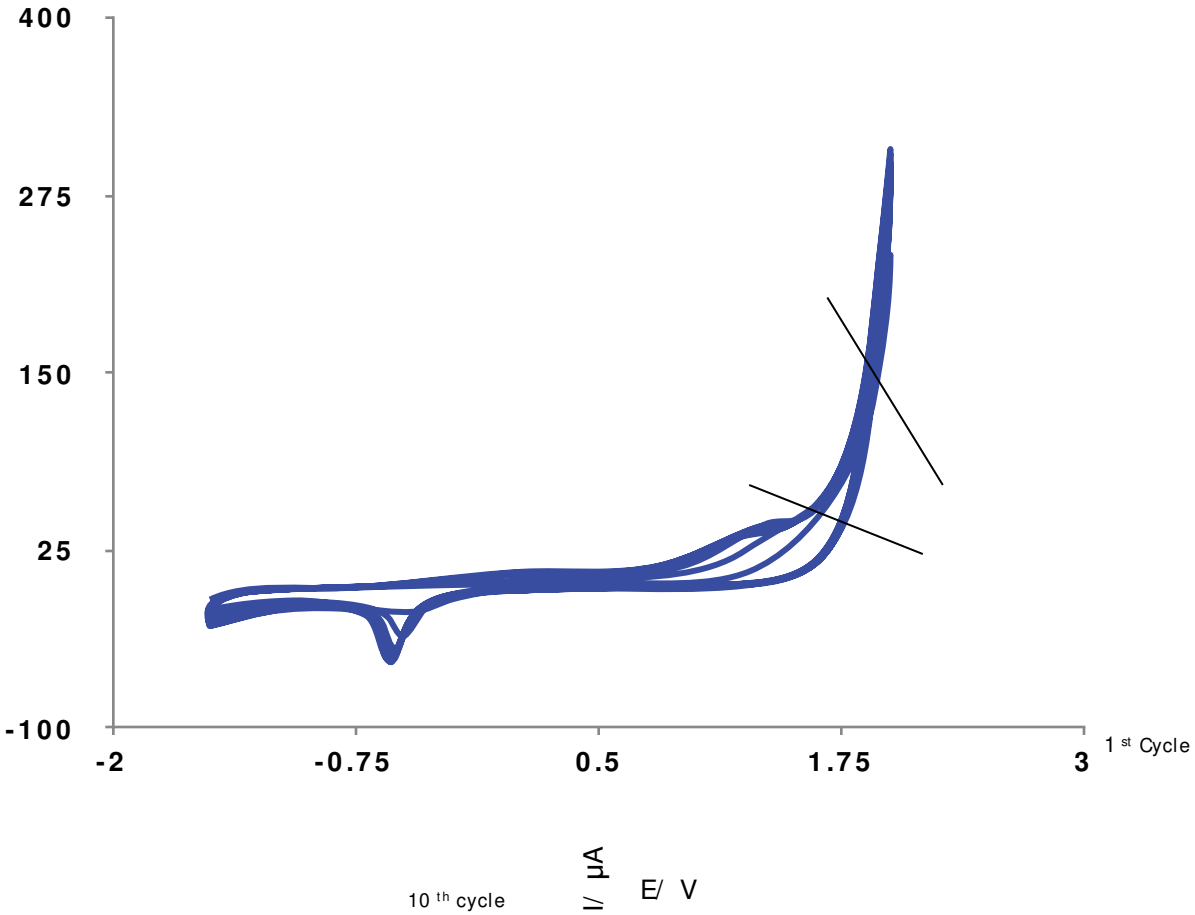

Fig. 1. Cyclic voltammograms for the electrochemical polymerization of 0.5 mM l-arginine on a GCE at the scan rate 100 mV/s. No. of cycle is 10.

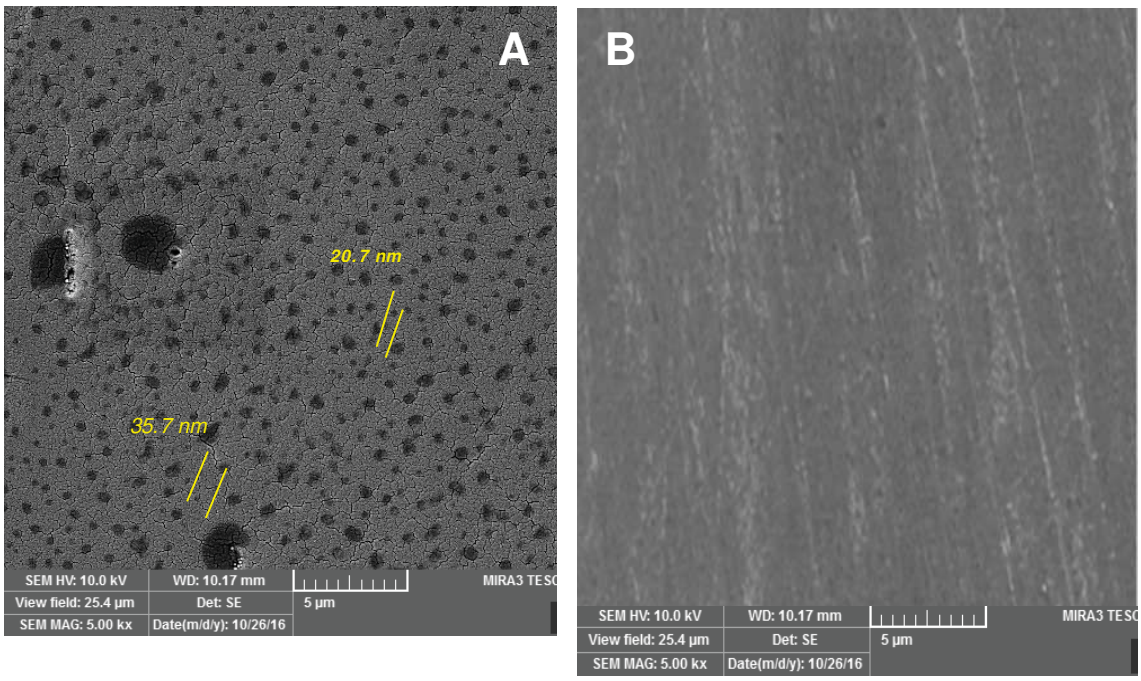

Fig. 2. FEG-SEM images of GCE (**A**) and PARG modified GCE (**B**).

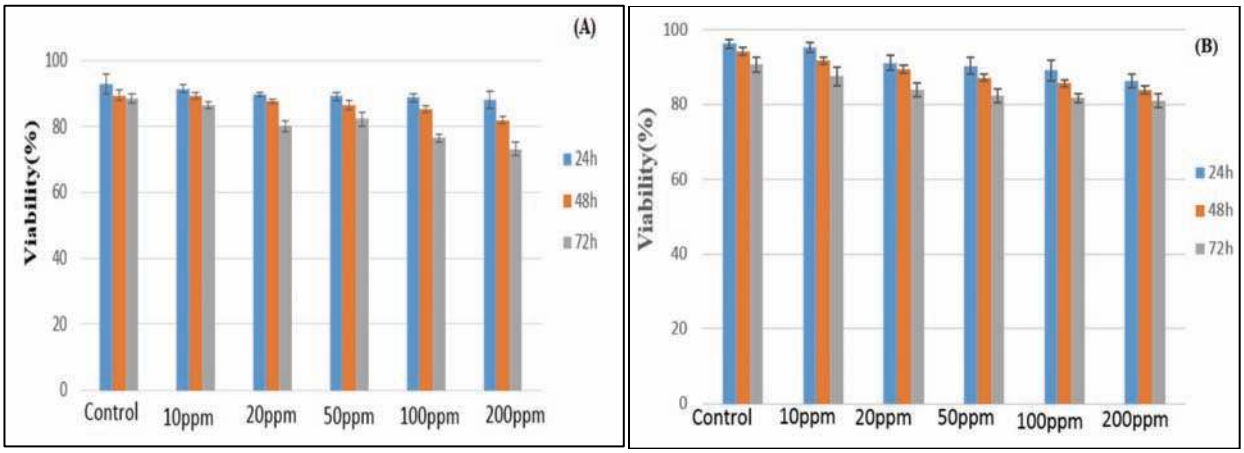

Fig. 3. GQDs induced cell death in (**A**) HepG2 cells and (**B**) non-tumorigenic cell line (NIH-3T3). Cells were treated with (0,10, 20, 50, 100 and 200 ppm GQDs for 24, 48 and 72 hours and cell viability was measured using MTT [3(4,5dimethylthiazol2yl) 2,5diphenyltetrazolium bromide] reduction assay. Data represent the mean ± S.E.M. (n = 6).

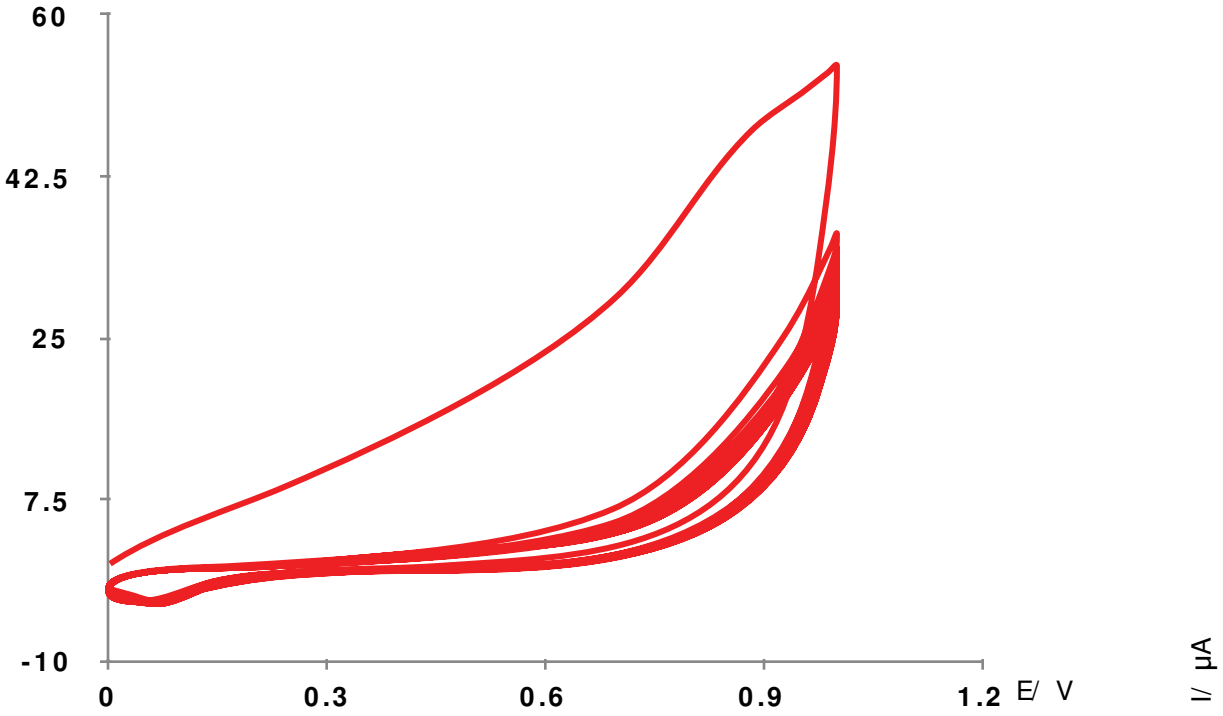

Fig. 4. Cyclic voltammograms for the electrodeposition of 0.002 g/mL GQDs on a GCE modified by PARG at the scan rate 100 mV/s. No. of cycle is 30.

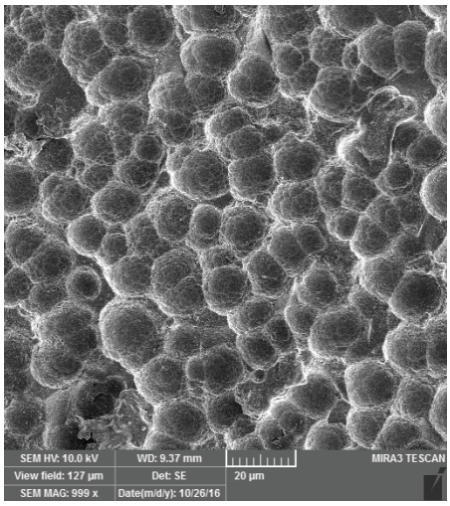
SEM HV: 10.0 kV
WD: 9.37 mm
MIRA3 TESCAN
View field: 127 µm
Det: SE
20 µm
SEM MAG: 999 x
Date(m/d/y): 10/26/16

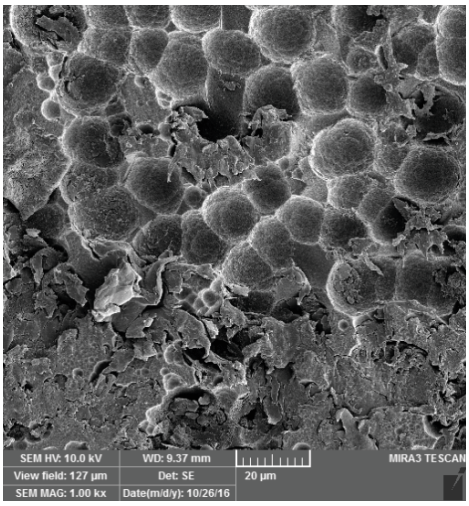
SEM HV: 10.0 kV
WD: 9.37 mm
MIRA3 TESCAN
View field: 127 µm
Det: SE
20 µm
SEM MAG: 1.00 kx
Date(m/d/y): 10/26/16

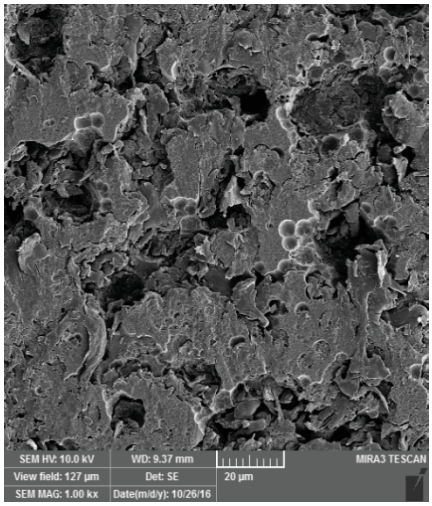
SEM HV: 10.0 kV
WD: 9.37 mm
MIRA3 TESCAN
View field: 127 µm
Det: SE
20 µm
SEM MAG: 1.00 kx
Date(m/d/y): 10/26/16

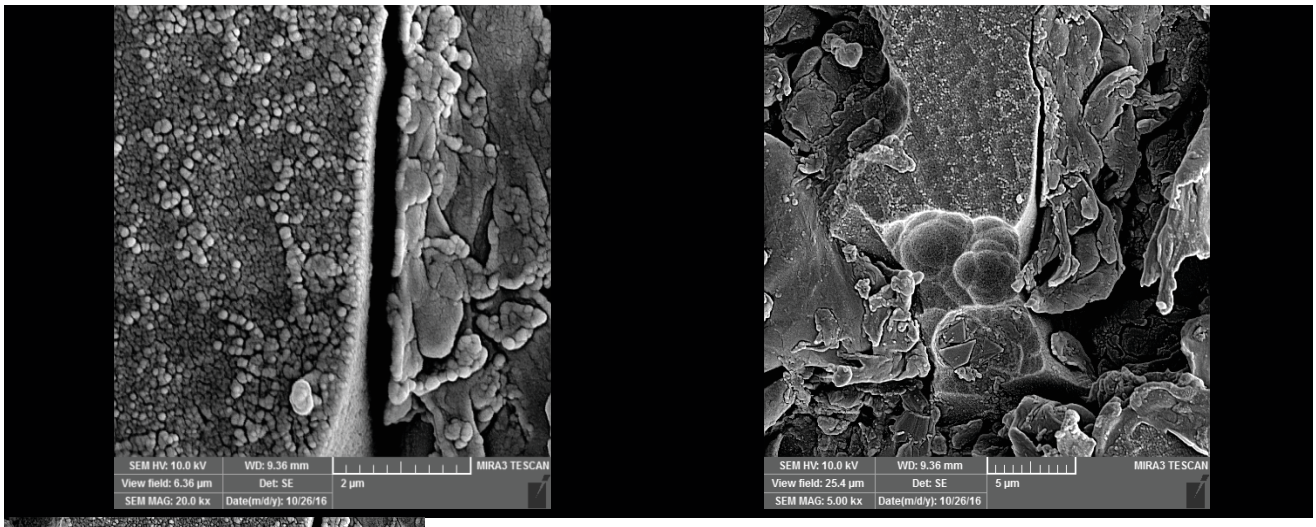
SEM HV: 10.0 kV
WD: 9.36 mm
MIRA3 TESCAN
View field: 6.36 µm
Det: SE
2 µm
SEM MAG: 20.0 kx
Date(m/d/y): 10/26/16
SEM HV: 10.0 kV
WD: 9.36 mm
MIRA3 TESCAN
View field: 25.4 µm
Det: SE
5 µm
SEM MAG: 5.00 kx
Date(m/d/y): 10/26/16

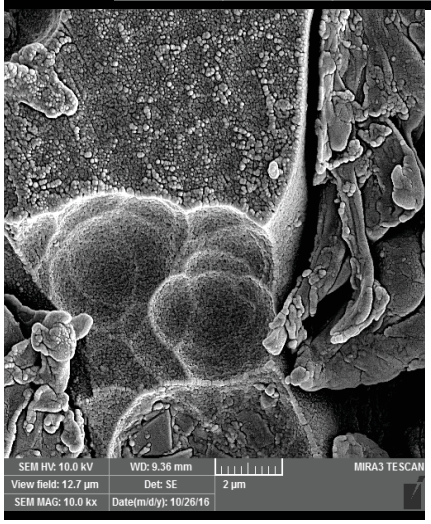
SEM HV: 10.0 kV
WD: 9.36 mm
MIRA3 TESCAN
View field: 12.7 µm
Det: SE
2 µm
SEM MAG: 10.0 kx
Date(m/d/y): 10/26/16

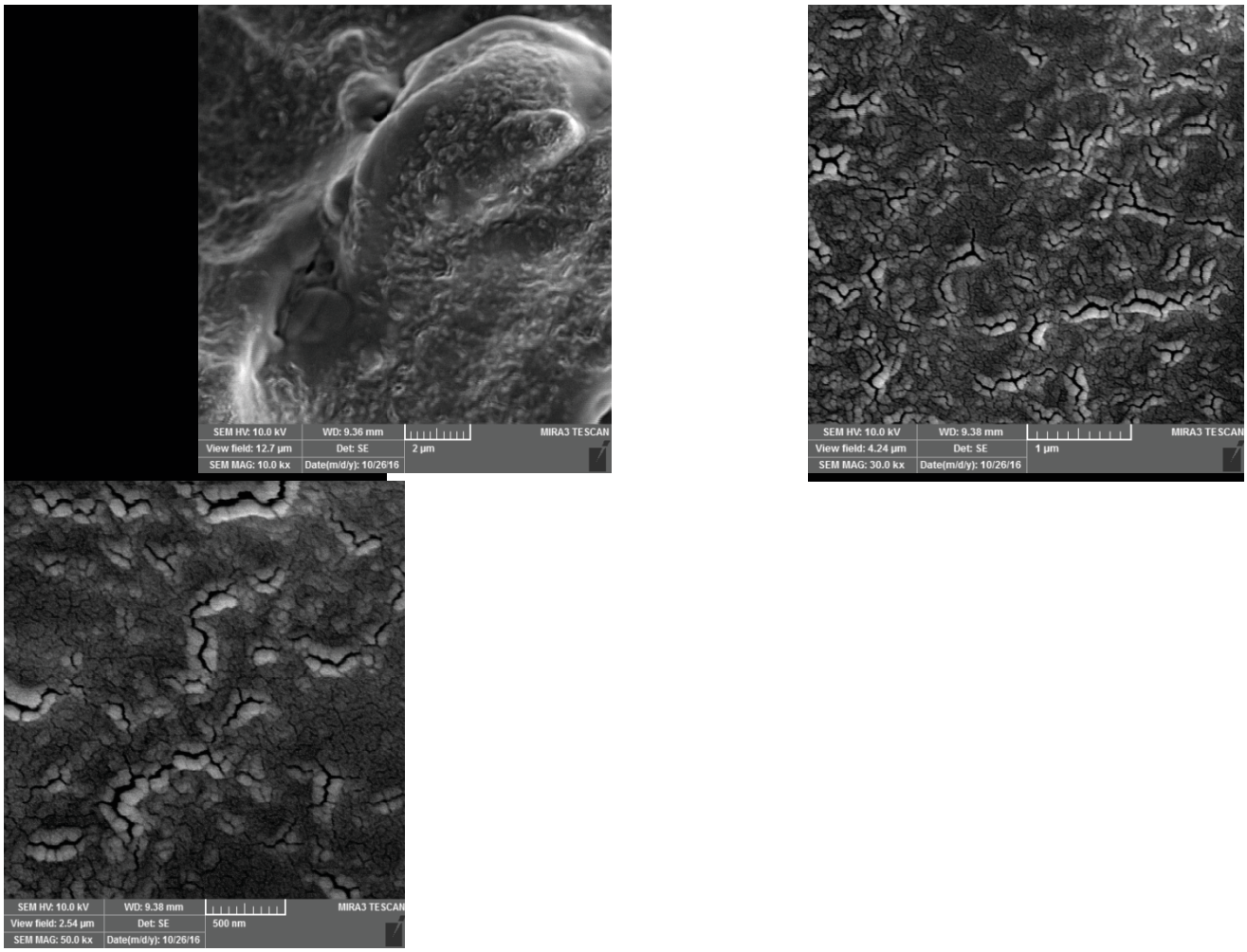

Fig. 5. FEG-SEM images of PARG-GQDs modified GCE in different magnitude.

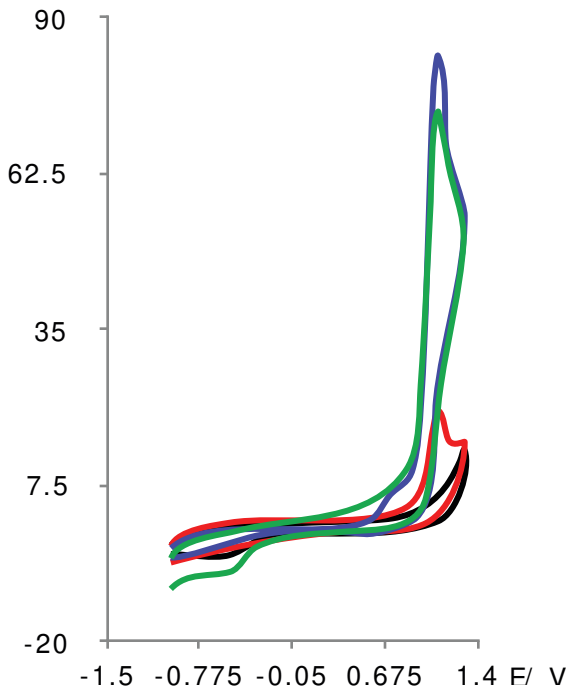

CV

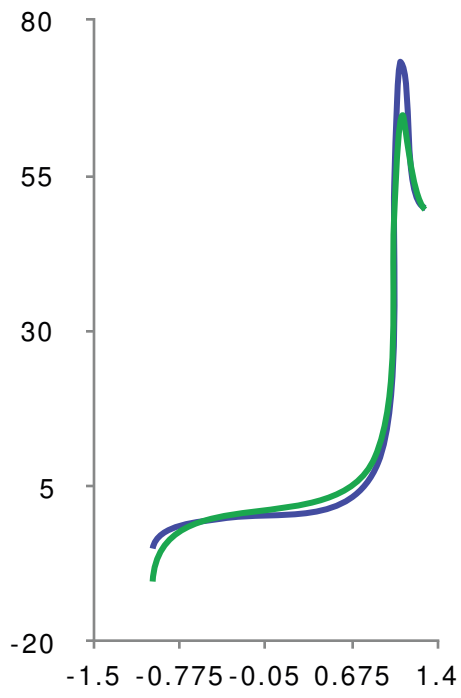

LSV

I/ µA F/ V

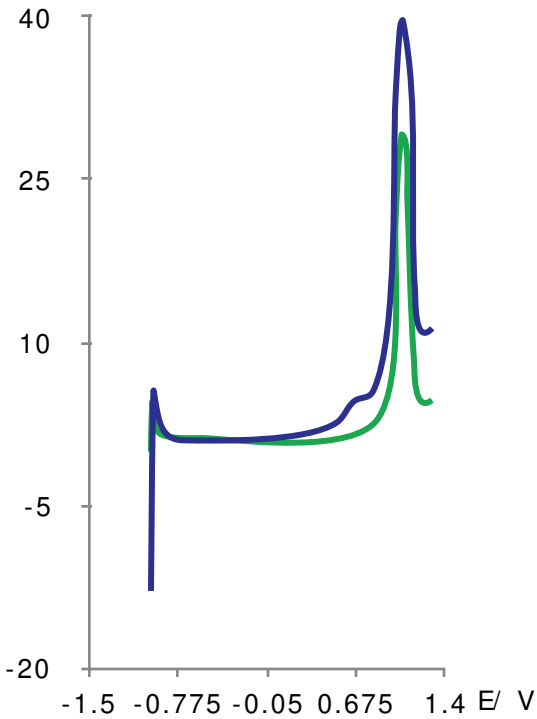

DPV

I/ µA

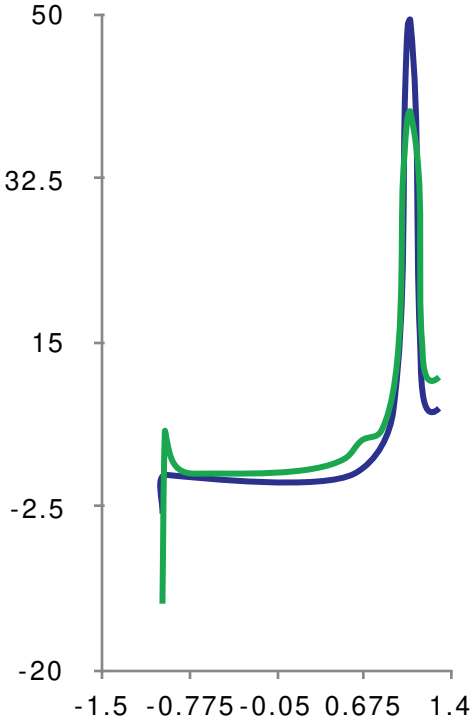

SWV

I/ µA E/ V

Fig. 6: (**A**) CVs of GCE (**Black** curve), GQDs-GCE (**Red** curve), PARG-GCE (**Green**) and PARG-GQDs-GCE (**Blue** curve) in PBS (pH=7.4) +MDA (0.1 mM); **B**) LSVs; **C**) DPVs and **D**) SWVs of PARG-GCE (**Green** curve) and PARG-GQDs-GCE (**Blue** curve) in PBS (pH=7.4) +MDA (0.1 mM).

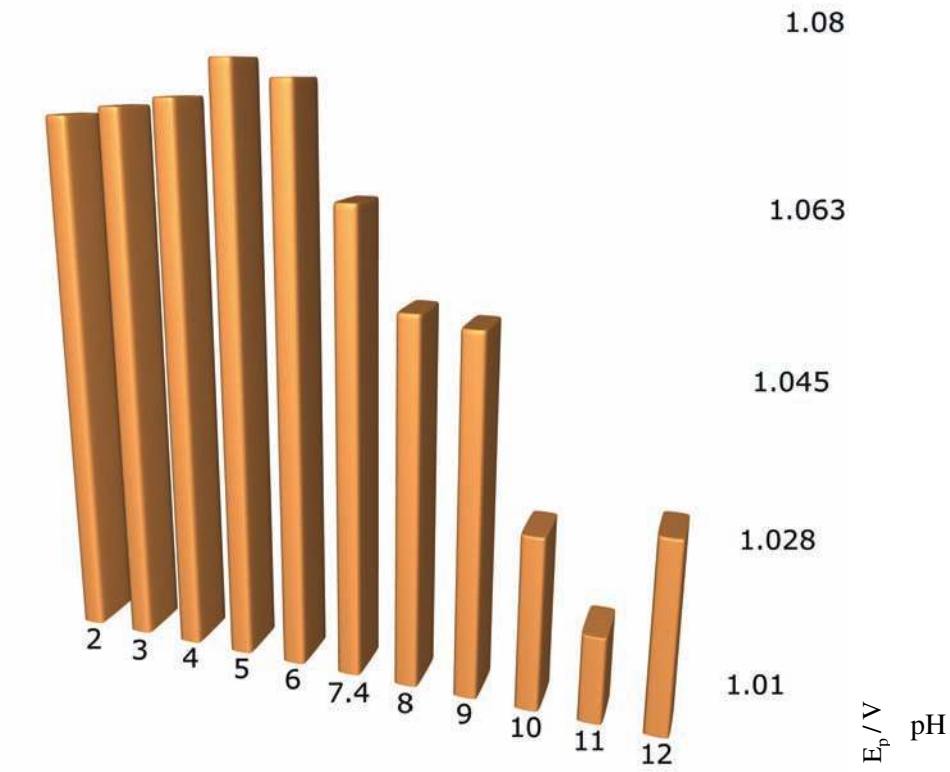

Fig. 7. The effect of pH on the electrooxidation of MDA using PARG-GQDs-GCE

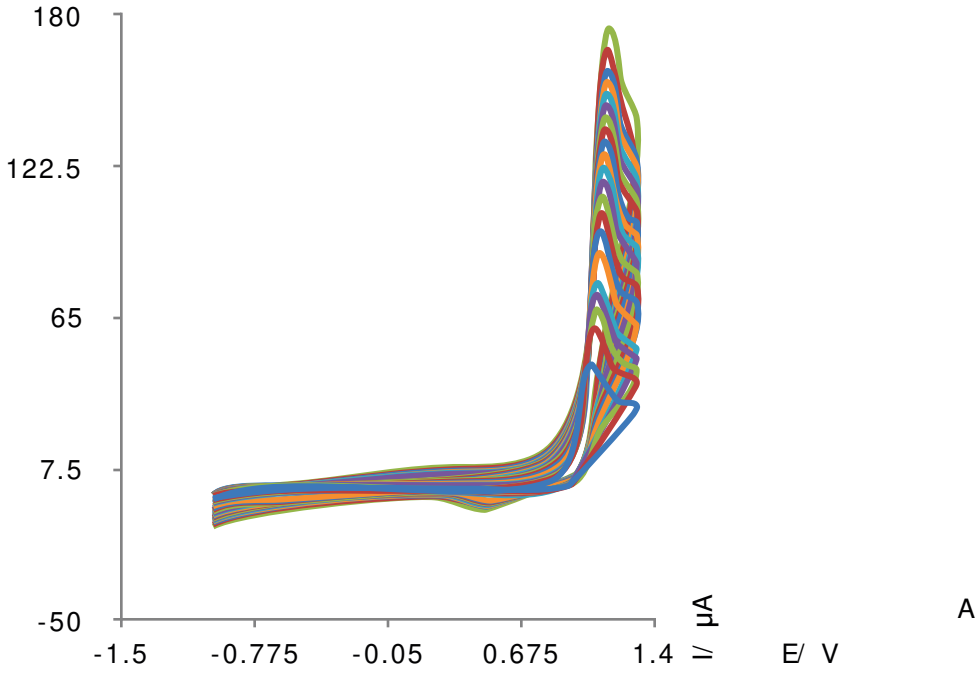
180
122.5
65
7.5
-50
-1.5
-0.775
-0.05
0.675
1.4
I/ µA
E/ V

A

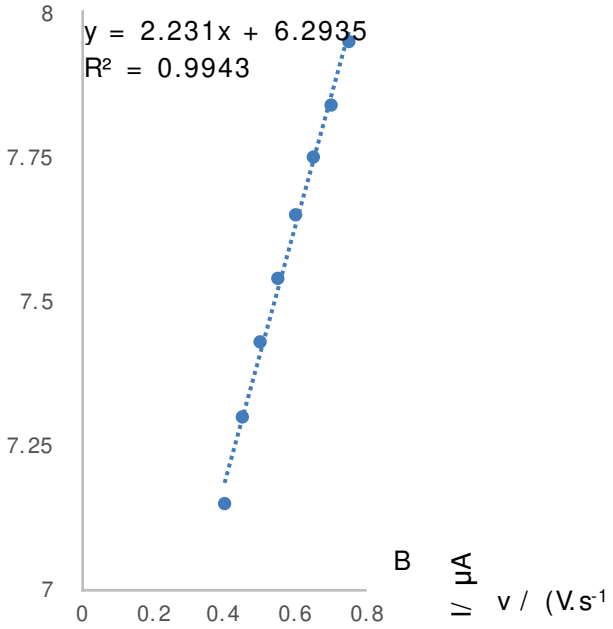
y = 2.231x + 6.2935
R² = 0.9943
8
7.75
7.5
7.25
7
0
0.2
0.4
0.6
0.8
I/ µA
v / (V.s-1

B

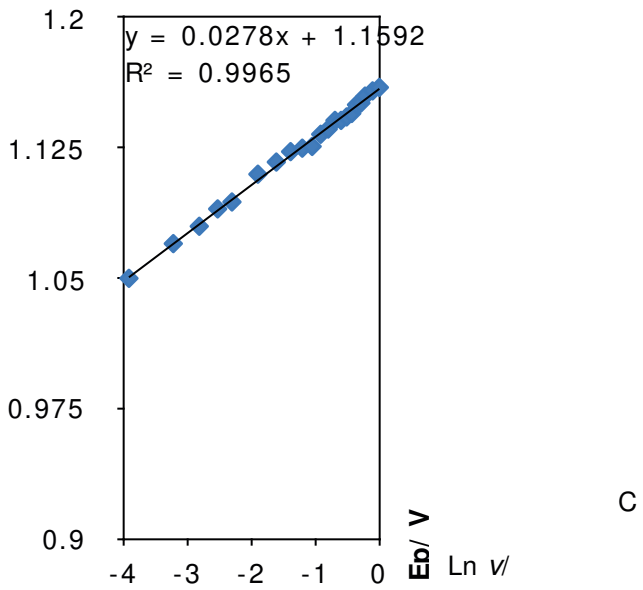

Fig. 8. **A**) CVs of PARG-GQDs-GCE in different scan rate (2, 5, 10, 25, 50, 60, 70, 80, 90, 100, 150, 200, 250, 300, 350, 400, 450, 500, 550, 600, 650, 700, 750, 800, 850, 900, 950 and 1000 mV/s) in the presence of 0.01 mM MDA; **B)** Variations of oxidation peak currents versus scan rate; **C**)) Variations of oxidation peak potential versus neperian logarithm of scan rate.

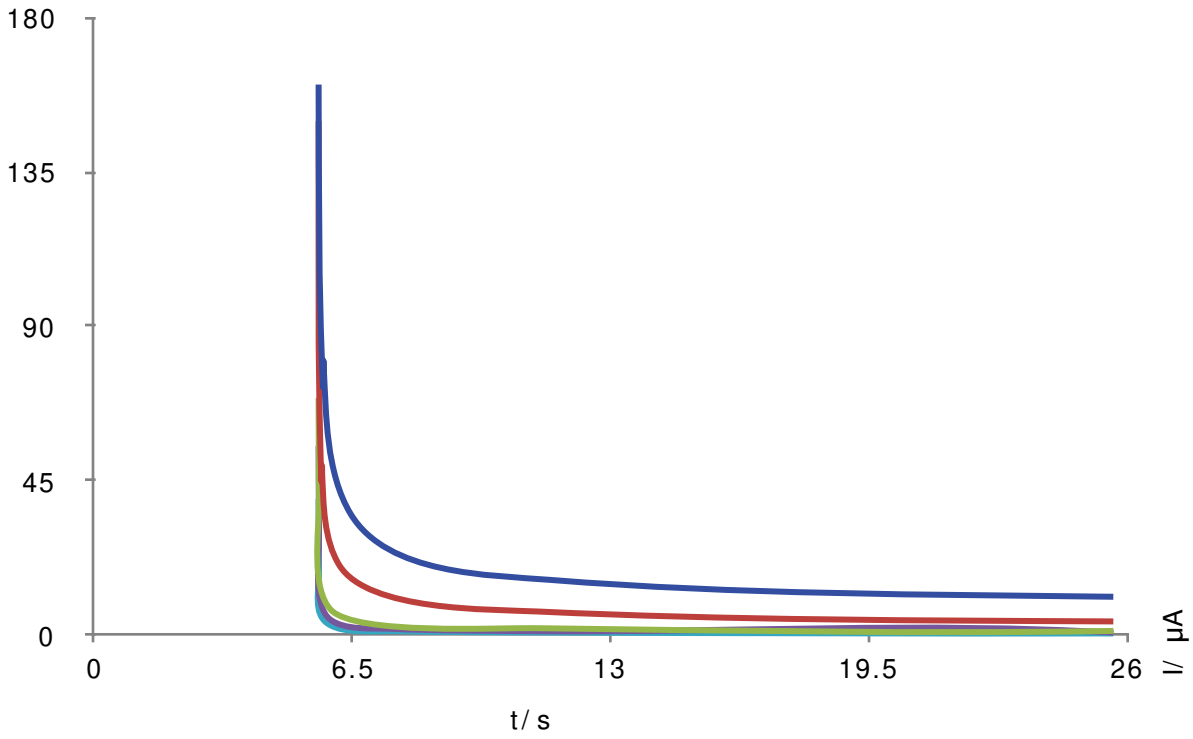

Fig. 9. Chronoamperograms of PARG-GQDs-GCE in different concentrations of MDA in the presence of 0.1M PBS (7.4)

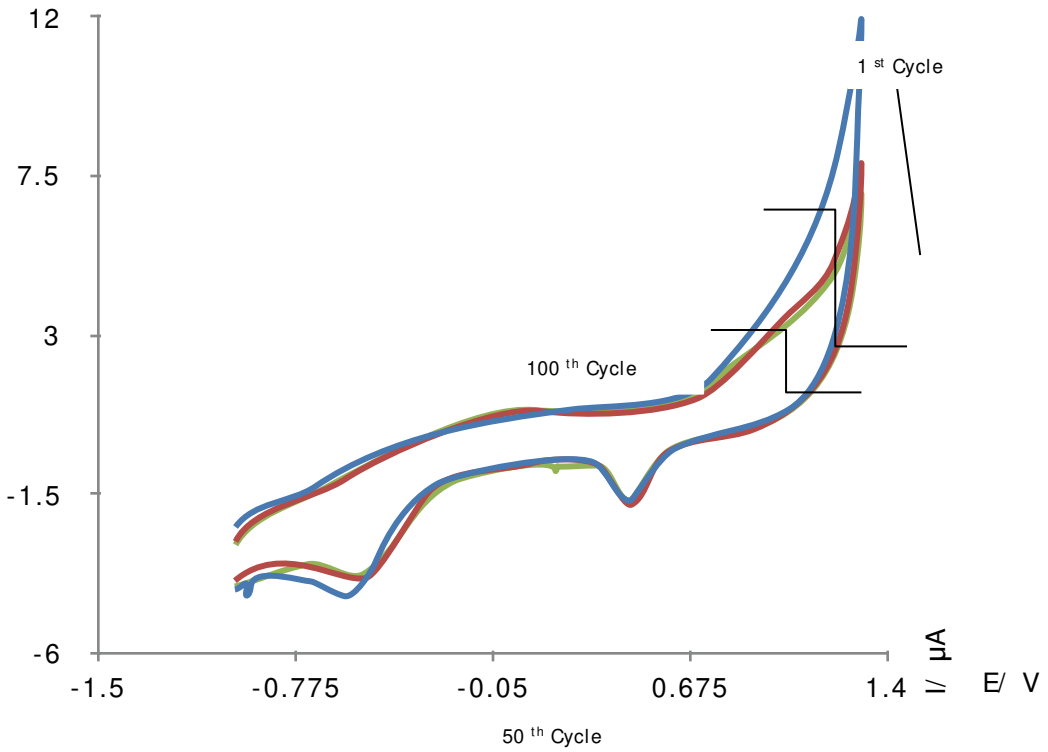

Fig. 10. GCE in different cycle numbers (1-100) in 0.01 PBS (pH 7.4)

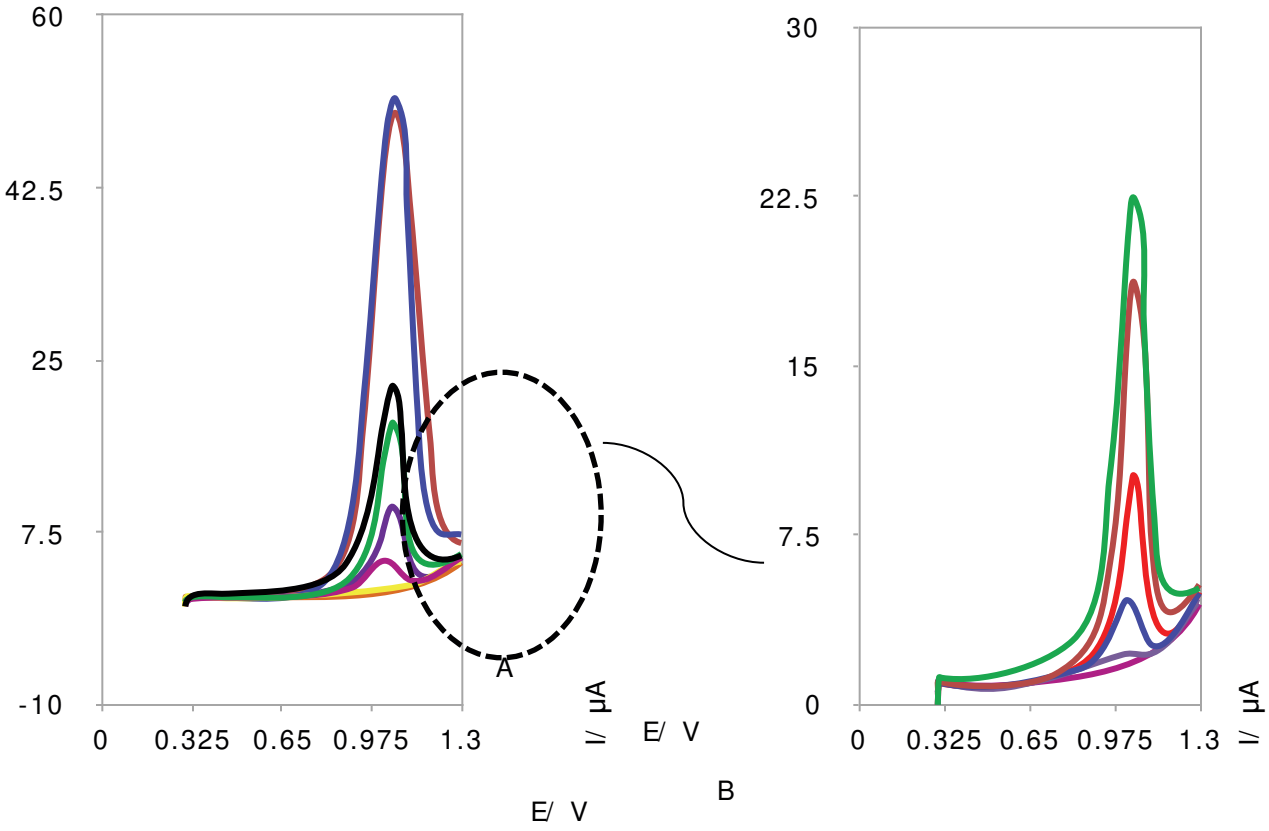

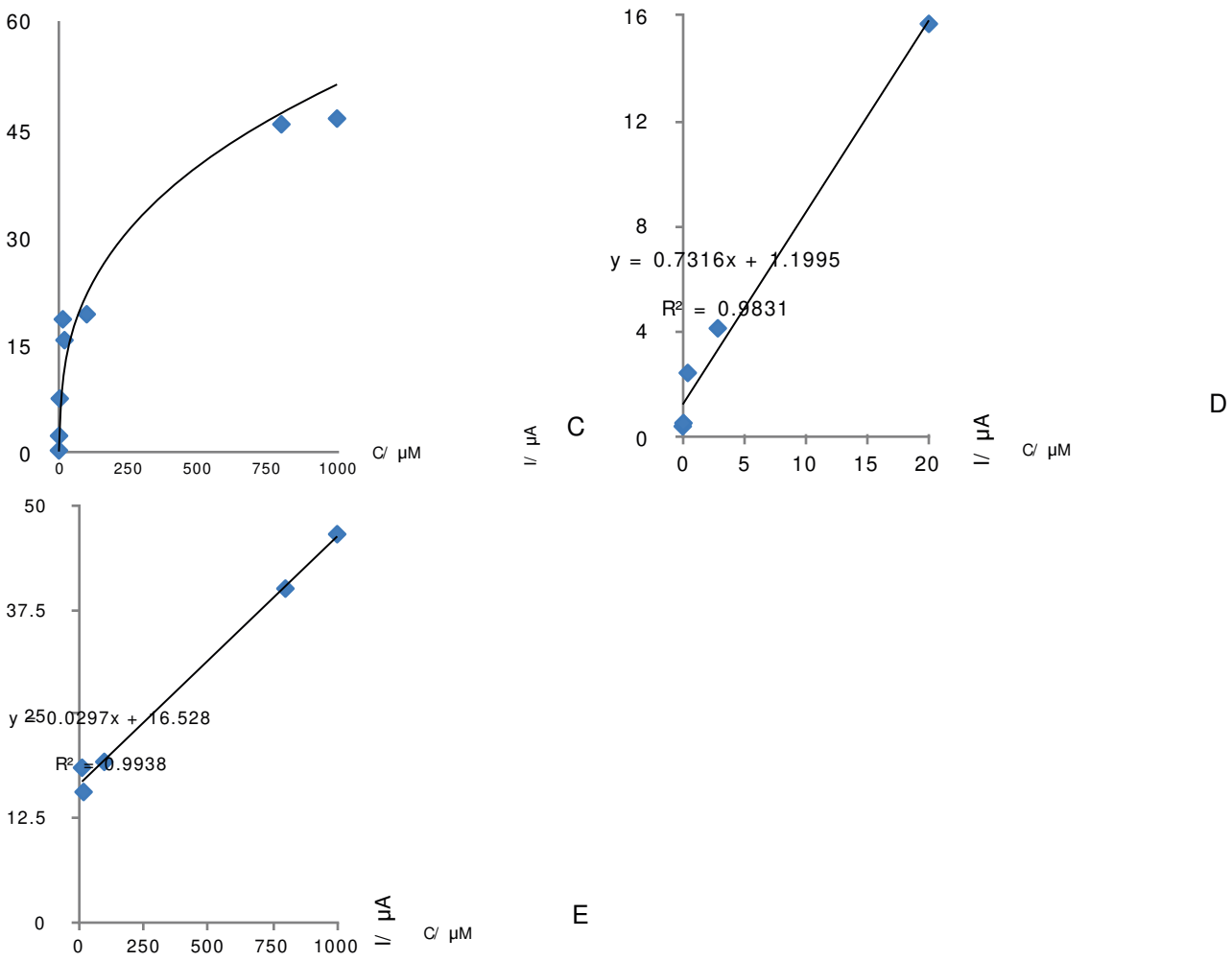

Fig. 11. **A**) DPVs obtained for determination of MDA in 0.1M PBS using PARG-GQDs-GCE. MDA concentrations are as: 0.000285, 0.0002, 0.00014, 0.001, 0.008, 0.01, 0.16, 0.18, and 0.1 mM. **B**) DPVs obtained for determination of MDA in low concentrations using PARG-GQDs-GCE. **C**) Calibration curve of MDA in above mentioned concentrations. **D**) Calibration curve of MDA in low concentrations; **E**) Calibration curve of MDA in high concentrations.

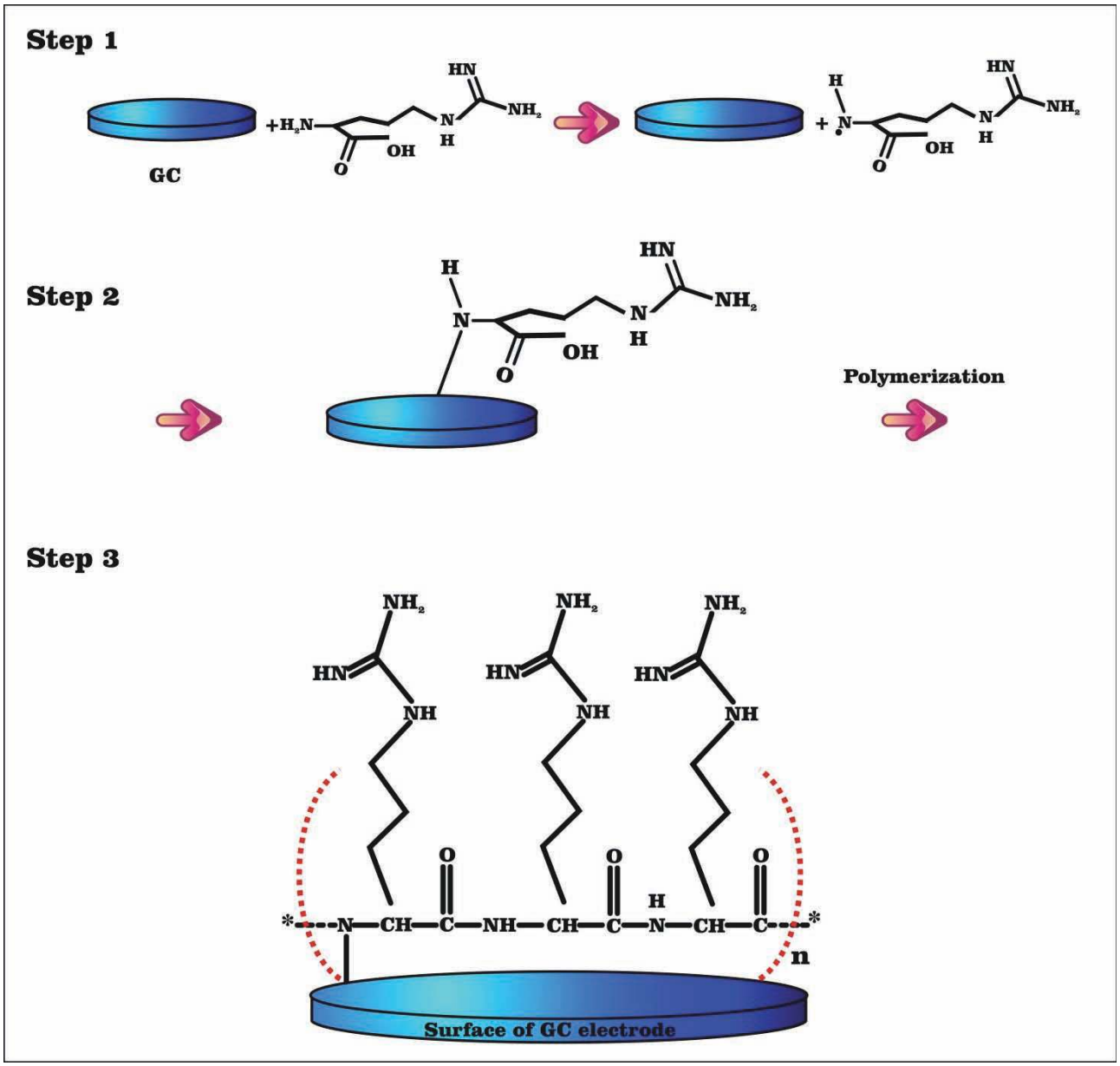

Scheme 1. Proposed mechanism of the preparation of PARG on the surface of GCE

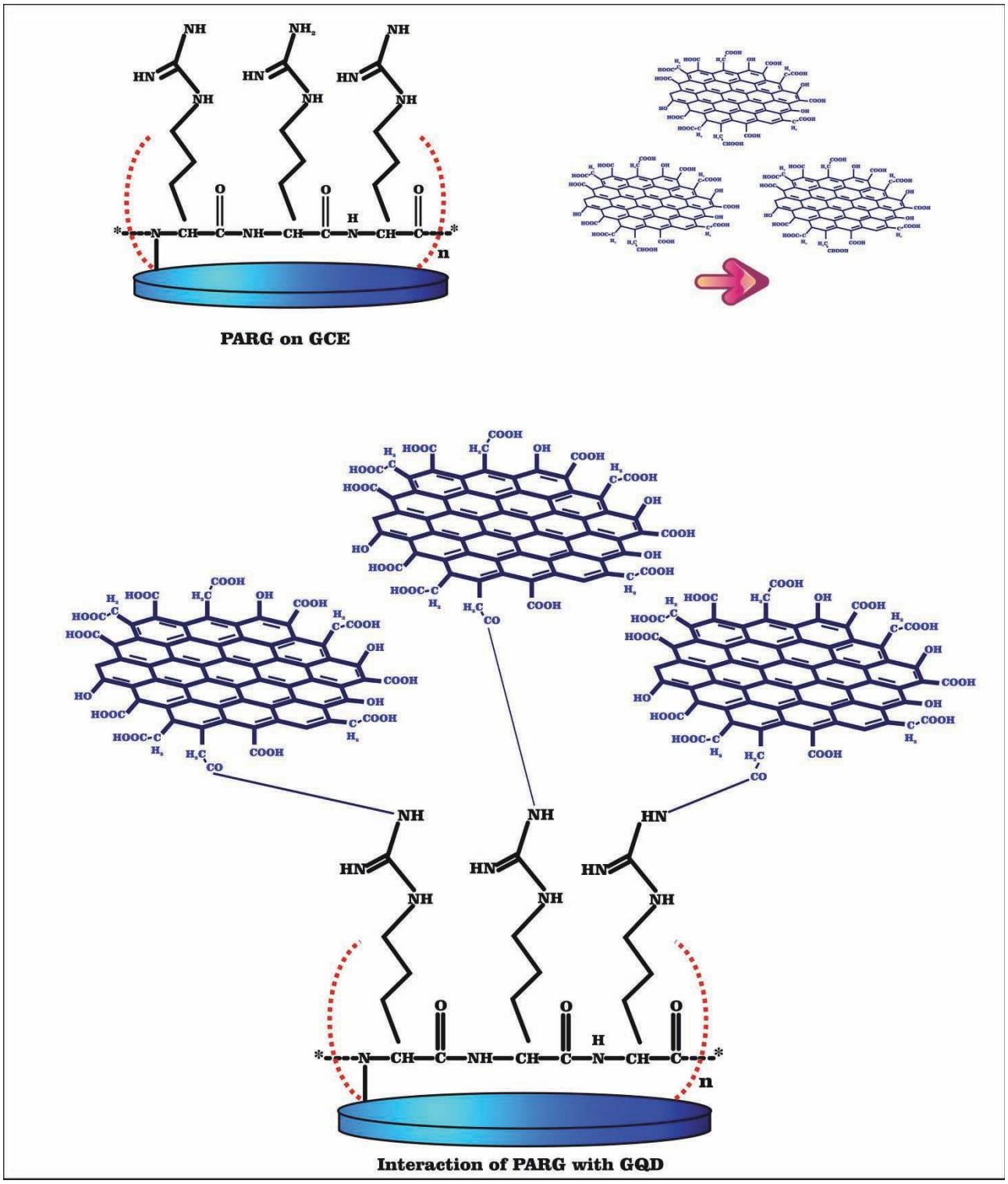

Scheme 2. Proposed mechanism of the preparation of PARG-GQDs on the surface of GCE.

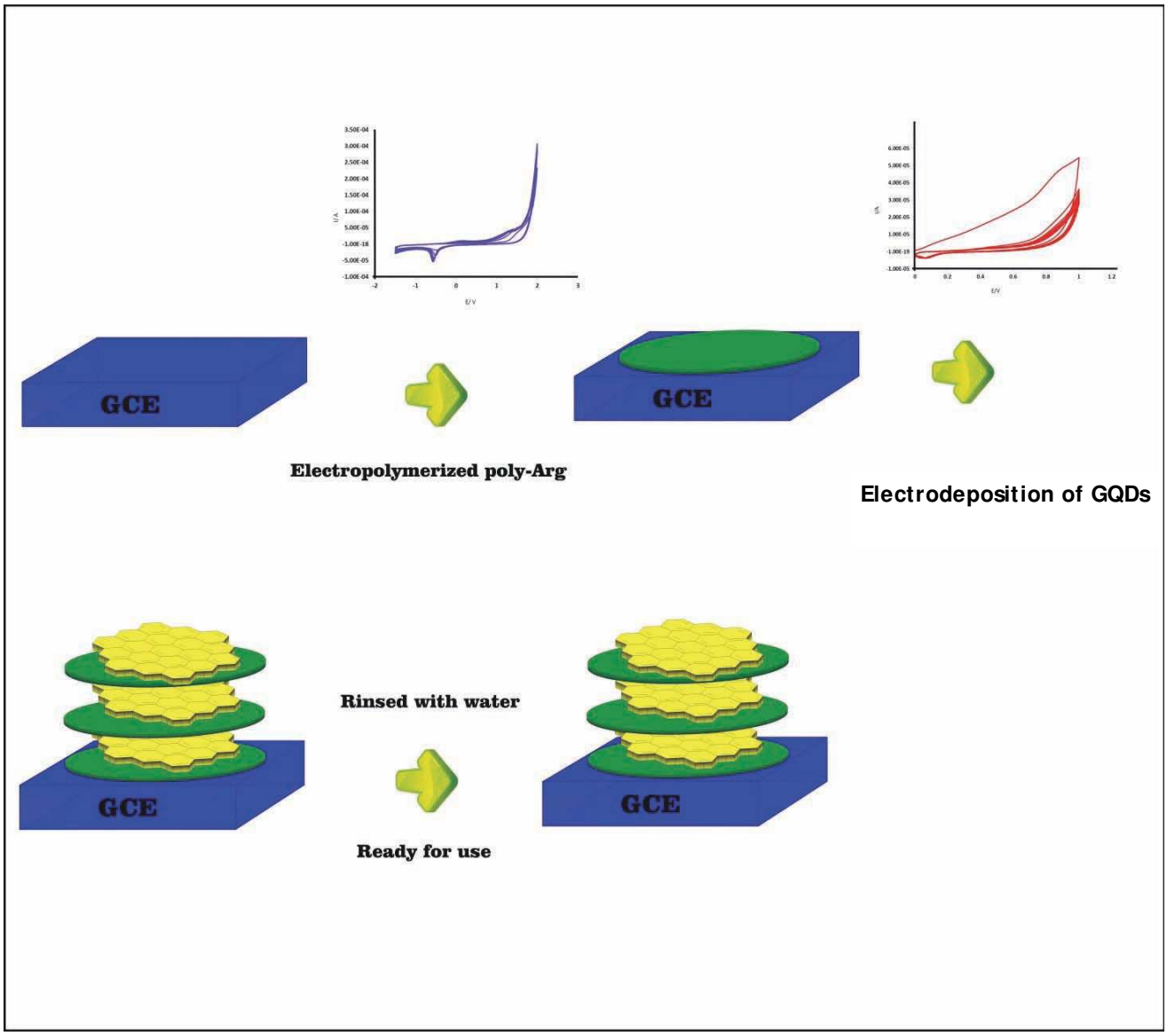

Scheme 3. Preparation steps of PARG-GQDs film on GCE surface

Table 1. Obtained results for detection of MDA in EBC sample standard addition method	
Concentration (µM)	**Signal [I /µA]**
26000	3.7
53	0.605
7.6	0.587

Table 2 compartment the results of MDA in EBC using the proposed and UV-vis methods in different samples

Sample No.	**MDA concentration**		
	This method	**UV-Vis**	**Relative error (%)**
1	1.32	-	-
2	1.78	-	-
3	5.50	8.22	26.39
4	10.23	15.60	30.21